

Mesoscopic electron and phonon transport through a curved wire

Shi-Xian Qu and Michael R. Geller

Department of Physics and Astronomy, University of Georgia, Athens, Georgia 30602-2451, USA

(Received 9 April 2004; published 26 August 2004)

There is great interest in the development of novel nanomachines that use charge, spin, or energy transport to enable new sensors with unprecedented measurement capabilities. Electrical and thermal transport in these mesoscopic systems typically involves wave propagation through a nanoscale geometry such as a quantum wire. In this paper we present a general theoretical technique to describe wave propagation through a curved wire of uniform cross section and lying in a plane, but of otherwise arbitrary shape. The method consists of (i) introducing a local orthogonal coordinate system, the arclength, and two locally perpendicular coordinate axes, dictated by the shape of the wire; (ii) rewriting the wave equation of interest in this system; (iii) identifying an effective scattering potential caused by the local curvature; and (iv) solving the associated Lippmann-Schwinger equation for the scattering matrix. We carry out this procedure in detail for the scalar Helmholtz equation with both hard-wall and stress-free boundary conditions, appropriate for the mesoscopic transport of electrons and (scalar) phonons. An interesting aspect of the phonon case is that the reflection probability always vanishes in the long-wavelength limit, allowing a simple perturbative (Born approximation) treatment at low energies. Our results show that, in contrast to charge transport, curvature only barely suppresses thermal transport, even for sharply bent wires, at least within the two-dimensional scalar phonon model considered. Applications to experiments are also discussed.

DOI: 10.1103/PhysRevB.70.085414

PACS number(s): 85.85.+j, 03.65.Nk, 63.22.+m, 73.23.-b

I. INTRODUCTION

A new class of nanomachines is attempting to measure extremely minute amounts of energy, of the order a few neV, and to use such calorimeters to probe fundamental properties of thermal conduction in the nanoscale regime.¹⁻⁵ Similar to the related case of electrical conduction,^{6,7} low-temperature thermal conduction in nanostructures is entirely different than in macroscopic materials because the phonons are in the mesoscopic regime, where they scatter elastically but not inelastically. Because inelastic scattering is required to establish thermodynamic equilibrium, there is a breakdown of Fourier's law and the heat equation, which assume a local thermodynamic equilibrium characterized by a spatially varying temperature profile. These nanodevices have inspired considerable theoretical work on thermal transport by phonons in the mesoscopic limit.⁸⁻²²

In this paper we introduce a general method to calculate the scattering matrix for waves propagating through a curved wire or waveguide. The wire is assumed to be of uniform cross section and lying in a plane, but the curved segment may have any smooth curvature profile,²³ such as that shown schematically in Fig. 1(a). The ends of the wire (the "leads") are also assumed to be straight. For definiteness we consider two-dimensional waves described by the scalar Helmholtz equation

$$[\nabla^2 + \alpha]\Phi(\mathbf{r}) = 0, \quad \mathbf{r} \equiv (x, y) \quad (1)$$

which is appropriate for electrons or scalar phonons in flat wires with rectangular cross section.²⁴ Here $\alpha(\epsilon) \equiv 2m\epsilon/\hbar^2$ in the case of electrons of energy ϵ and mass m , whereas $\alpha(\epsilon) \equiv \epsilon^2/\hbar^2v^2$ in the case of scalar phonons of energy ϵ and bulk sound velocity v . Electron spin is of no importance here

and is neglected. The boundary conditions at the edges of the wire are

$$\Phi(\mathbf{r}) = 0 \quad (\text{for electrons}),$$

$$\mathbf{n} \cdot \nabla \Phi(\mathbf{r}) = 0 \quad (\text{for phonons}), \quad (2)$$

where $\mathbf{n}(\mathbf{r})$ is a local outward-pointing normal. Here we have assumed conventional hard-wall boundary conditions for the electronic states, but stress-free conditions for the elastic

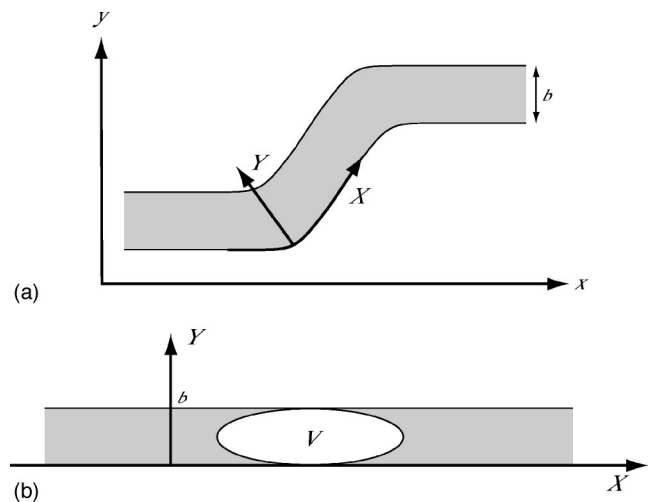


FIG. 1. (a) An example of the type of two-dimensional curved wire geometry considered in this paper. The shape of the wire is used to define local orthogonal coordinates X and Y , with X the arclength along one of the edges. The width of the wire is b . (b) Scattering problem in the XY frame. Here the wire appears straight, but the curvature induces an effective potential V that causes scattering.

waves because in this case the wires are usually freely suspended.

Although the wave equation in Eq. (1) is certainly simple, the scattering problem described here is complicated because the boundary conditions (2) are applied along the curves defining the two edges of the wire. Our approach involves rewriting Eqs. (1) and (2) in terms of new curvilinear coordinates X and Y , dictated by the shape of the wire, such that the wave equation becomes more complicated (the wire's curvature produces an effective potential), but the boundary conditions become trivial. We choose X to be the arclength along one edge of the wire, and Y is locally perpendicular. This transformation allows us to apply the standard techniques of scattering theory, including solution of the Lippmann-Schwinger equation, in the XY frame.

A particularly novel aspect of the phonon transport problem is that the reflection probability always vanishes in the long-wavelength limit, permitting an analytic (second-order Born approximation) treatment at low energies. The energy-dependent transmission probability is then expressed as a simple functional of the curvature profile $\kappa(X)$, making possible a straightforward analysis of a variety of wire shapes. The fact that long-wavelength phonons have perfect transmission is a consequence of the rigid-body nature of the underlying system: An elastic wave with infinite wavelength is just an adiabatic rigid translation of the wire, which must transmit energy perfectly.

There has been considerable attention given to mesoscopic electron transport through curved wires and wave guides,²⁵ but none to thermal transport. Electron transmission probabilities in curved wires are usually obtained by mode matching, a method restricted to piecewise separable geometries (wires composed of straight segments, circles, and other shapes where the wave equation is separable). A related problem that has been studied extensively is the formation of electronic bound states and resonances in curved wires, where the mapping to local curvilinear coordinates is also often used.²⁵⁻²⁷ Surprisingly, we are not aware of any work using moving frames and then directly solving the resulting Lippmann-Schwinger equation in that basis.²⁸ Nor are we aware of the use of this method in the extensive microwave engineering literature,^{29,30} where the (more generally applicable but purely numerical) finite-element method is the technique of choice.

In the next section we carry out the above analysis for the two-dimensional Helmholtz equation. In Sec. III we consider electron transport through a circular right-angle bend, recovering results obtained by Sols and Macucci³¹ and by Lin and Jaffe³² using mode-matching methods. Our main results are given in Sec. IV, where we address thermal transport through curved wires. Section V contains a discussion of our conclusions and the experimental implications of this work.

II. APPLICATION TO SCALAR WAVE EQUATION

We now explain our method in detail and apply it to the scalar scattering problem stated in Eqs. (1) and (2).

A. Curvilinear coordinate system

First we use the shape of the wire to define a curvilinear coordinate system, the arclength X along one edge and a

locally perpendicular coordinate Y . Which edge one chooses is of course arbitrary. The direction of increasing Y will be chosen so that X, Y , and z form a right-handed coordinate system. Both edges are assumed to be a smooth plane curves.²³

The unit tangent vector

$$\mathbf{e}_X \equiv \frac{d\mathbf{r}}{dX} = \frac{dx}{dX}\mathbf{e}_x + \frac{dy}{dX}\mathbf{e}_y \quad (3)$$

and normal

$$\mathbf{e}_Y \equiv -\frac{dy}{dX}\mathbf{e}_x + \frac{dx}{dX}\mathbf{e}_y \quad (4)$$

define local orthonormal basis vectors for the XY frame. The sign in Eq. (4) is chosen so that $\mathbf{e}_X \times \mathbf{e}_Y = \mathbf{e}_z$. We then use the Frenet-Serret equation

$$\frac{d\mathbf{e}_X}{dX} = \kappa(X)\mathbf{e}_Y \quad (5)$$

to define a signed curvature $\kappa(X)$ of the $Y=0$ edge. According to this definition, $\kappa(X)$ is positive when Y increases toward the center of curvature. We will also make use of the metric tensor

$$g = \begin{bmatrix} (1 - \kappa Y)^2 & 0 \\ 0 & 1 \end{bmatrix} \quad (6)$$

in the XY system.

B. Helmholtz equation in curvilinear coordinates

Next we make a coordinate transformation from \mathbf{r} to $\mathbf{R} \equiv (X, Y)$, and rewrite the wave equation in terms of these coordinates. A convenient way to do this is to use the identity

$$\nabla^2 = (\det g)^{-1/2} \frac{\partial}{\partial X_i} (\det g)^{1/2} g_{ij}^{-1} \frac{\partial}{\partial X_j}. \quad (7)$$

The Helmholtz equation (1) then becomes

$$[\partial_X^2 + \partial_Y^2 - V + \alpha]\Phi(\mathbf{R}) = 0, \quad (8)$$

where we have separated the combination $\partial_X^2 + \partial_Y^2$ from the many terms that appear on the right-hand side of Eq. (7), and combined the remaining ones into an effective potential V . The potential V is itself a differential operator; an explicit expression will be given below. The boundary conditions (2) are now

$$\Phi(\mathbf{R}) = 0 \quad (\text{for electrons}),$$

$$\partial_Y \Phi(\mathbf{R}) = 0 \quad (\text{for phonons}) \quad (9)$$

on the edges $Y=0$ and $Y=b$, with b the width of the wire. A scattering state $\Phi(\mathbf{R})$ becomes fully determined once we specify its behavior as $X \rightarrow \pm\infty$.

In the XY frame the wire appears straight, as illustrated in Fig. 1(b). The scattering potential vanishes in the leads because the wire is straight there. We are now able to use conventional scattering theory.

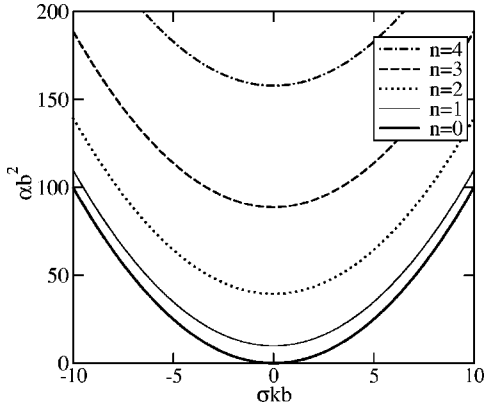


FIG. 2. Dispersion relation for unperturbed scattering states, for both spinless electrons and scalar phonons. α is equal to $2m\epsilon/\hbar^2$ in the case of electrons, or ϵ^2/\hbar^2v^2 in the case of phonons. σ is 1 on the right half of the figure, and -1 on the left. b is the wire width.

C. Unperturbed scattering states

The unperturbed ($V=0$) scattering states for both spinless electrons and scalar phonons are labeled by three quantum numbers σ , n , and ϵ , and can be written in the form

$$\phi_{\sigma n \epsilon}(\mathbf{R}) = c_{n \epsilon} e^{\sigma i k_n \epsilon X} \chi_n(Y), \quad (10)$$

where

$$k_{n \epsilon} \equiv \sqrt{\alpha(\epsilon) - (n\pi/b)^2} \quad (11)$$

is the wave number along the wire,

$$\chi_n(Y) \equiv \begin{cases} \sqrt{2/b} \sin(n\pi Y/b) & \text{for electrons,} \\ \sqrt{(2 - \delta_{n0})/b} \cos(n\pi Y/b) & \text{for phonons} \end{cases} \quad (12)$$

is a trigonometric function satisfying the transverse boundary conditions of Eq. (9), and

$$c_{n \epsilon} \equiv \frac{1}{\sqrt{2\pi}} \left| \frac{\partial k_{n \epsilon}}{\partial \epsilon} \right|^{1/2} \quad (13)$$

is a real normalization constant. σ is a chirality index, defined by

$$\sigma \begin{cases} +1 & \text{if moving in the } +X \text{ direction} \\ -1 & \text{if moving in the } -X \text{ direction} \end{cases}, \quad (14)$$

and n is an integer-valued branch index. The transverse eigenfunctions $\chi_n(Y)$ are normalized according to

$$\int_0^b dY \chi_n(Y) \chi_{n'}(Y) = \delta_{nn'}. \quad (15)$$

The dispersion relation given by Eq. (11) is shown in Fig. 2.

The allowed values of the quantum numbers σ , n , and ϵ are as follows: The allowed energies form a continuum, from ϵ_{\min} to ∞ . Here

$$\epsilon_{\min} \equiv \begin{cases} \frac{\hbar^2 \pi^2}{2mb^2} & \text{for electrons,} \\ 0 & \text{for phonons.} \end{cases} \quad (16)$$

For each value of energy, the branch index takes the values in a set S of integers defined by

$$S \equiv \begin{cases} 1, 2, \dots, N & \text{for electrons,} \\ 0, 1, 2, \dots, N & \text{for phonons,} \end{cases} \quad (17)$$

where

$$N(\epsilon) \equiv \sum_{n=0}^{\infty} \Theta \left[\alpha(\epsilon) - \frac{n^2 \pi^2}{b^2} \right] - 1, \quad (18)$$

with $\Theta(x)$ the unit step function. For electrons, N is the number of propagating channels below energy ϵ , whereas for phonons the number of propagating channels is $N+1$. Finally, for each allowed value of ϵ and n , σ takes on the values ± 1 .

The free scattering states satisfy the orthonormality and completeness conditions

$$\int d^2R \phi_{\sigma n \epsilon}^*(\mathbf{R}) \phi_{\sigma' n' \epsilon'}(\mathbf{R}) = \delta_{\sigma \sigma'} \delta_{nn'} \delta(\epsilon - \epsilon') \quad (19)$$

and

$$\int_{\epsilon_{\min}}^{\infty} d\epsilon \sum_{\sigma=\pm 1} \sum_{n \in S} \phi_{\sigma n \epsilon}^*(\mathbf{R}) \phi_{\sigma n \epsilon}(\mathbf{R}') = \delta(\mathbf{R} - \mathbf{R}'), \quad (20)$$

where n takes the values given in Eq. (17).

D. Effective potential

The terms $\partial_X^2 + \partial_Y^2$ have been separated out from the right-hand side of Eq. (7) so that the eigenfunctions $\Phi(\mathbf{R})$ reduce to that of a straight wire when $V=0$. Accordingly, the effective potential is given by

$$V = \frac{\kappa^2 Y^2 - 2\kappa Y}{(1 - \kappa Y)^2} \partial_X^2 - \frac{\kappa' Y}{(1 - \kappa Y)^3} \partial_X + \frac{\kappa}{1 - \kappa Y} \partial_Y. \quad (21)$$

There will be no singularities in V as long as

$$-\infty < \kappa b < 1. \quad (22)$$

The condition (22) guarantees that both the $Y=0$ and $Y=b$ edges of the wire are smooth.

In applications where the radius of curvature $|\kappa|^{-1}$ is much larger than b , Eq. (21) can be simplified. To leading order in κb the effective potential reduces to

$$V = -2\kappa Y \partial_X^2 - \kappa' Y (1 + 3\kappa Y) \partial_X + \kappa \partial_Y. \quad (23)$$

E. Lippmann-Schwinger equation

The scattering problem in the XY frame can be solved by standard methods. The Lippmann-Schwinger equation for an eigenfunction $\Phi(\mathbf{R})$ with (electron or phonon) energy ϵ is

$$\Phi(\mathbf{R}) = \phi_{\text{in}}(\mathbf{R}) + \int d^2R' G_0(\mathbf{R}, \mathbf{R}', \epsilon) V \Phi(\mathbf{R}'), \quad (24)$$

where $\phi_{\text{in}}(\mathbf{R})$ is a free scattering state coming in from the left, and where $G_0(\mathbf{R}, \mathbf{R}', \epsilon)$ is the Green's function for the unperturbed Helmholtz equation, satisfying

$$[\partial_X^2 + \partial_Y^2 + \alpha(\epsilon)] G_0(\mathbf{R}, \mathbf{R}', \epsilon) = \delta(\mathbf{R} - \mathbf{R}'), \quad (25)$$

along with the boundary condition that $G_0(\mathbf{R}, \mathbf{R}', \epsilon)$ vanishes as $|X - X'| \rightarrow \infty$. The Lippmann-Schwinger equation gives the solution of Eq. (8) subject to the condition that $\Phi(\mathbf{R})$ reduces to the incident state $\phi_{\text{in}}(\mathbf{R})$ when $X \rightarrow -\infty$.

The unperturbed Green's function for both electrons and phonons is

$$G_0(\mathbf{R}, \mathbf{R}', \epsilon) = -\frac{i}{2} \sum_{n=0}^{\infty} \frac{\chi_n(Y) \chi_n(Y')}{k_{n\epsilon}} e^{ik_{n\epsilon}|X-X'|}. \quad (26)$$

We note that the summation in Eq. (26) is *not* restricted to the values given in Eq. (17). In particular, off-shell values of $k_{n\epsilon}$ are included. Furthermore, in the electron case the $n=0$ term in the summation vanishes, because the transverse eigenfunction $\chi_0(Y)$ vanishes.

We will also need to write Eq. (24) in the alternative form

$$\Phi(\mathbf{R}) = \phi_{\text{in}}(\mathbf{R}) + \int d^2R' G(\mathbf{R}, \mathbf{R}', \epsilon) V \phi_{\text{in}}(\mathbf{R}'), \quad (27)$$

where $G(\mathbf{R}, \mathbf{R}', \epsilon)$ is the Green's function of the *perturbed* Helmholtz equation, satisfying

$$G(\mathbf{R}, \mathbf{R}', \epsilon) = G_0(\mathbf{R}, \mathbf{R}', \epsilon) + \int d^2R'' G_0(\mathbf{R}, \mathbf{R}'', \epsilon) V G(\mathbf{R}'', \mathbf{R}', \epsilon). \quad (28)$$

F. Transmission probability

The transmission coefficient matrix $t_{nn'}(\epsilon)$ gives the probability amplitude for a right-moving electron or phonon to forward scatter from branch n to branch n' at energy ϵ . We define $t_{nn'}(\epsilon)$ to be zero if one or both branches have minima above ϵ .

We can obtain a formal expression for $t_{nn'}(\epsilon)$ by writing the $X \rightarrow \infty$ limit of the unperturbed Green's function as

$$G_0(\mathbf{R}, \mathbf{R}', \epsilon) \rightarrow -\frac{i}{2} \sum_{n \in S} \frac{\phi_{Rn\epsilon}(\mathbf{R}) \phi_{Rn'\epsilon}^*(\mathbf{R}')}{k_{n\epsilon} c_{n\epsilon}^2}, \quad (29)$$

where the subscripts R denote right-moving ($\sigma = +1$) waves. The summation in Eq. (29) is now restricted to $n \leq N$ because the higher lying contributions are exponentially small in the $X \rightarrow \infty$ limit. Then from Eqs. (24) and (29) we obtain

$$\lim_{X \rightarrow \infty} \Phi(\mathbf{R}) = \phi_{Rn_i\epsilon}(\mathbf{R}) - \frac{i}{2} \sum_{n \in S} \frac{\langle \phi_{Rn\epsilon} | V | \Phi \rangle}{k_{n\epsilon} c_{n\epsilon}^2} \phi_{Rn\epsilon}(\mathbf{R}), \quad (30)$$

where the incoming right-moving wave is assumed to be in channel n_i . Therefore we conclude that

$$\lim_{X \rightarrow -\infty} \Phi = \phi_{Rn_i\epsilon} \quad (31)$$

and

$$\lim_{X \rightarrow \infty} \Phi = \sum_{n \in S} t_{nn'}(\epsilon) \phi_{Rn\epsilon}, \quad (32)$$

where

$$t_{nn'}(\epsilon) \equiv \delta_{nn'} - \frac{i \langle \phi_{Rn'\epsilon} | V | \Phi \rangle}{k_{n'\epsilon} c_{n'\epsilon}^2} \quad (33)$$

is the amplitude for an incident wave (R, n, ϵ) to forward scatter to (R, n', ϵ) . $t_{nn'}(\epsilon)$ is called the transmission matrix.

We emphasize that for the case of electron transport, $t(\epsilon)$ is an $N \times N$ matrix, where N varies with energy as indicated in Eq. (18). For phonons, $t(\epsilon)$ is $N+1$ dimensional.

The expectation value in Eq. (33) involves the exact scattering state Φ with boundary condition corresponding to an incident state (R, n, ω) . Using Eq. (27) we write this as

$$\begin{aligned} \langle \phi_{Rn'\epsilon} | V | \Phi \rangle &= \langle \phi_{Rn'\epsilon} | V | \phi_{Rn\epsilon} \rangle \\ &+ \int \phi_{Rn'\epsilon}^*(\mathbf{R}) V_R G(\mathbf{R}, \mathbf{R}', \epsilon) V_{R'} \phi_{Rn\epsilon}(\mathbf{R}'), \end{aligned} \quad (34)$$

where V_R and $V_{R'}$ act on \mathbf{R} and \mathbf{R}' , respectively. The numerical method we use consists of expressing Eq. (28) in a basis of unperturbed scattering states, solving this equation by matrix inversion, and using Eq. (34) to obtain the transmission matrix in Eq. (33).

Finally, we define the energy-dependent transmission probabilities T_{el} and T_{ph} for electrons and phonons that determine the electrical and thermal currents. For electrons, the relevant quantity is the ratio of transmitted to incident charge current, given by

$$T_{\text{el}}(\epsilon) = \sum_{n, n'=1}^N |t_{nn'}|^2 = \text{Tr } t^\dagger t. \quad (35)$$

For thermal transport by phonons, the relevant quantity is the fraction of transmitted energy current,¹¹ given by

$$T_{\text{ph}}(\epsilon) = \sum_{n, n'=0}^N \frac{v_{n'}}{v_n} |t_{nn'}|^2, \quad (36)$$

where $v_n(\epsilon)$ is the phonon *group* velocity in the straight wire, which can be written as $\hbar v^2 k_{n\epsilon} / \epsilon$. Because the bulk sound velocity v is a constant here, and the scattering is elastic, we can equivalently write Eq. (36) as

$$T_{\text{ph}}(\epsilon) = \sum_{n, n'=0}^N \frac{k_{n'\epsilon}}{k_{n\epsilon}} |t_{nn'}|^2, \quad (37)$$

with the $k_{n\epsilon}$ given by Eq. (11).

G. Landauer formula

The charge current I and linear conductance

$$G \equiv \lim_{V \rightarrow 0} \frac{I}{V} \quad (38)$$

are related to the electron transmission probability $T_{\text{el}}(\epsilon)$ through the Landauer formula^{6,7}

$$I = \frac{e}{2\pi\hbar} \int_0^\infty d\epsilon T_{\text{el}}(\epsilon) [n_F^{\mu_l}(\epsilon) - n_F^{\mu_r}(\epsilon)]. \quad (39)$$

Here $n_F^{\mu_l}(\epsilon)$ and $n_F^{\mu_r}(\epsilon)$ are the Fermi distribution functions in the left (l) and right (r) leads, with chemical potentials μ_l and μ_r , differing in proportion to the applied voltage $V = (\mu_l - \mu_r)/e$.

Similarly, the thermal current I_{th} and conductance

$$G_{\text{th}} \equiv \lim_{\Delta T \rightarrow 0} \frac{I_{\text{th}}}{\Delta T} \quad (40)$$

are determined by the phonon transmission probability $T_{\text{ph}}(\epsilon)$ according to⁹⁻¹¹

$$I_{\text{th}} = \frac{1}{2\pi\hbar} \int_0^\infty d\epsilon \epsilon T_{\text{ph}}(\epsilon) [n_B^{T_l}(\epsilon) - n_B^{T_r}(\epsilon)]. \quad (41)$$

$n_B^{T_l}(\epsilon)$ and $n_B^{T_r}(\epsilon)$ are Bose distribution functions in the left and right leads, with temperatures T_l and T_r .

III. ELECTRON TRANSPORT

We turn now to an application of our method to coherent electron transport through a circular right-angle bend with outer radius R and width b . In this case the curvature profile is

$$\kappa(X) = \frac{1}{R} \Theta(X) \Theta\left(\frac{\pi R}{2} - X\right), \quad (42)$$

where Θ is the unit step function. The origin of the X coordinate is taken to be one of the locations where the straight and curved sections of the wire meet.

As explained above, the numerical method we use to calculate $t_{nn'}(\epsilon)$ requires the matrix elements $\langle \phi_{\sigma n} | V | \phi_{\sigma' n'} \rangle$ of the effective potential (21) in the unperturbed scattering states (10). However, matrix elements of the second term in Eq. (21), which contain the curvature gradient

$$\kappa'(X) = \frac{1}{R} \left[\delta(X) - \delta\left(X - \frac{\pi R}{2}\right) \right], \quad (43)$$

involves integrals of a delta function δ times functions $F(\Theta)$ of Θ . Integrals of this form, involving products of generalized functions, have to be evaluated carefully, as we show in Appendix A. Apart from this technicality, the application of our method to this geometry is straightforward.

Mesoscopic charge transport through bent wires has already been studied extensively,²⁵ and we will only consider one case of this, namely, $R = 1.2b$. First we calculate the individual electron transmission probabilities $|t_{nn'}(\epsilon)|^2$ from Eq. (33) for the lowest few channels n and n' . The results are given in Fig. 3 and are in excellent agreement with the mode-matching results of Sols and Macucci³¹ for the same

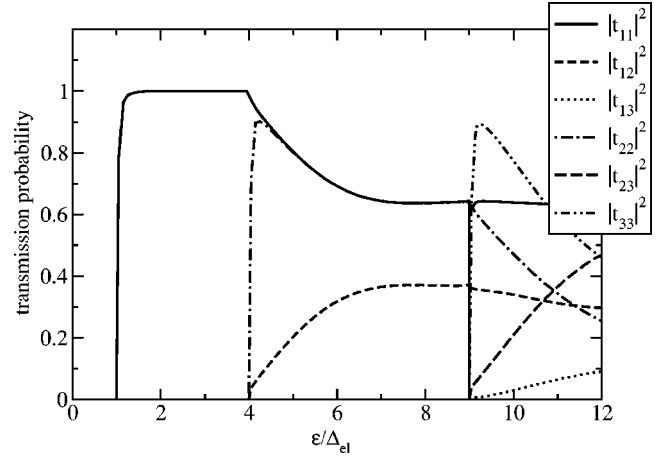


FIG. 3. Individual electron transmission probabilities $|t_{nn'}|^2$ as a function of energy for a circular right-angle bend with $R/b = 1.20$. Here $\Delta_{\text{el}} \equiv \pi^2 \hbar^2 / 2mb^2$.

value of R/b [see Fig. 2(a) of Ref. 31]. Our result for $|t_{11}(\epsilon)|^2$ also agrees qualitatively with that calculated by Lin and Jaffe³² for a right-angle bend with a slightly larger curvature- (see Fig. 8 of Ref. 32).

The total electron transmission probability $T_{\text{el}}(\epsilon)$, defined in Eq. (35), is presented in Fig. 4 for the same curved wire. At energies given by

$$\epsilon = n^2 \Delta_{\text{el}} \quad \text{with } n = 1, 2, 3, \dots, \quad (44)$$

where $\Delta_{\text{el}} \equiv \pi^2 \hbar^2 / 2mb^2$, additional channels in the wire become propagating and contribute to the transmission probability. The threshold energies (44) follows from Eq. (11) and Fig. 2. The principal effect of the curvature in the wire is to soften the transitions at these thresholds.

IV. PHONON TRANSPORT

We turn now to the main emphasis of our work, the calculation of transmission probabilities for two-dimensional scalar phonons with energy $\epsilon = \hbar\omega$ and (bulk) sound velocity v to propagate through curved wires. We are not aware of any previous work on this problem.

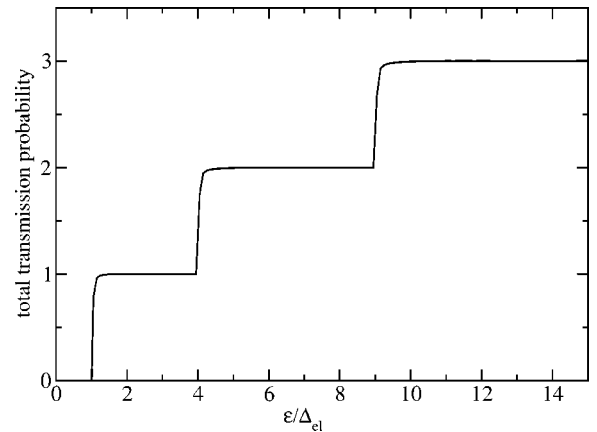


FIG. 4. Total electron transmission probability T_{el} . System parameters are the same as in Fig. 3.

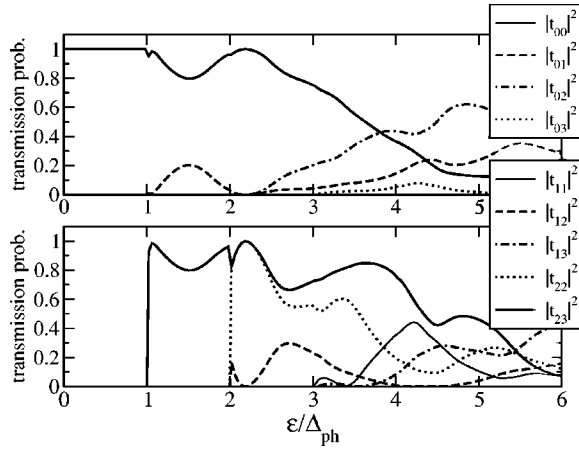


FIG. 5. Individual phonon transmission probabilities $|t_{nm'}|^2$ as a function of energy for a circular right-angle bend with $R=2b$. Here $\Delta_{\text{ph}} \equiv \pi\hbar v/b$.

As before, we consider a circular right-angle bend with outer radius R and width b , with curvature profile given by Eq. (42). The method of solution is the same as that outlined in Sec. III and Appendix A, except that the transverse parts of the unperturbed scattering states, defined in Eq. (12), are now different.

In Fig. 5 we give the individual phonon transmission probabilities $|t_{nm'}(\epsilon)|^2$, defined in Eq. (33), for the lowest channels in a smoothly bent wire with $R=2b$. In Fig. 6 we do the same for a more tightly bent wire, with $R=1.001b$ (inner radius is $10^{-3}b$). At energies given by

$$\epsilon = n\Delta_{\text{el}} \quad \text{with } n = 1, 2, 3, \dots, \quad (45)$$

where $\Delta_{\text{ph}} \equiv \pi\hbar v/b$, additional channels in the wire become propagating and contribute to thermal transport.

In both examples, transmission is nearly perfect in the low-energy limit, $\epsilon < \Delta_{\text{ph}}$ limit, where there is only a single propagating channel. At higher energies, scattering does occur. However it is mostly in the forward direction, and the fraction of transmitted energy $\mathbb{T}_{\text{ph}}(\epsilon)$, defined in Eq. (36), is essentially unchanged from that of a straight wire.

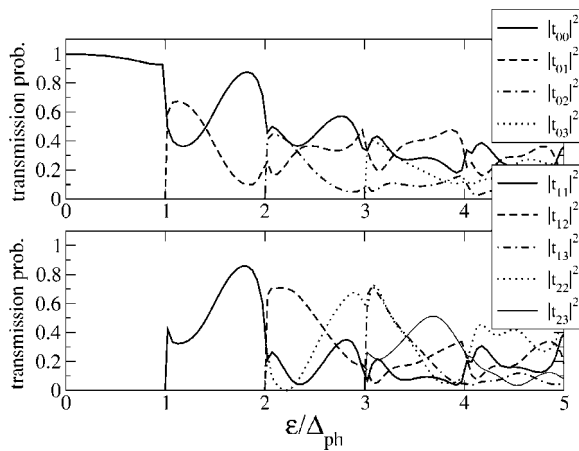


FIG. 6. Individual phonon transmission probabilities $|t_{nm'}|^2$ as a function of energy for a circular right-angle bend with $R=1.001b$.

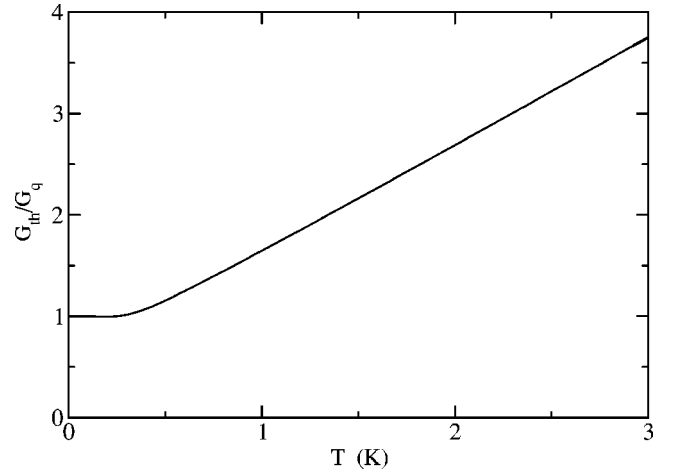


FIG. 7. Dimensionless thermal conductance G_{th}/G_q as a function of temperature, for a 100 nm curved Si-like quantum wire, with outer radius $R=1.001b$. Here $G_q \equiv \pi k_B^2 T/6\hbar$, which is itself linearly proportional to temperature.

In Fig. 7 we plot the thermal conductance G_{th} in units of the “quantum” of thermal conductance

$$G_q \equiv \frac{\pi k_B^2 T}{6\hbar} \approx 0.95T \text{ pW K}^{-2}, \quad (46)$$

for a curved wire of width $b=100$ nm and outer radius $R=1.001b$. The scalar phonon velocity is taken to be $v=8.5 \times 10^5 \text{ cm s}^{-1}$, the longitudinal sound speed in Si. The thermal transport is hardly affected by the curvature in the wire, as can be seen in Fig. 8, which compares an expanded plot of G_{th}/G_q to that for a straight wire. The greatest suppression occurs near 200 mK and is only about 0.5% of the thermal conductance quantum.

It is physically unrealistic to consider a 100 nm wire bent more sharply than $R=1.001b$, because the inner radius of 0.10 nm in this case is already approaching atomic dimensions. However, for a wire of width $b=10 \mu\text{m}$ and the same

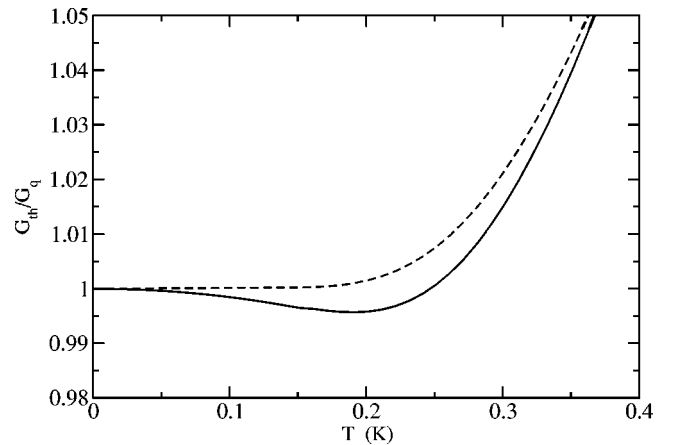


FIG. 8. The solid curve is the same as Fig. 7. Dashed curve is the dimensionless thermal conductance for a straight Si-like wire with $b=100$ nm. Thermal transport is hardly suppressed by the bending.

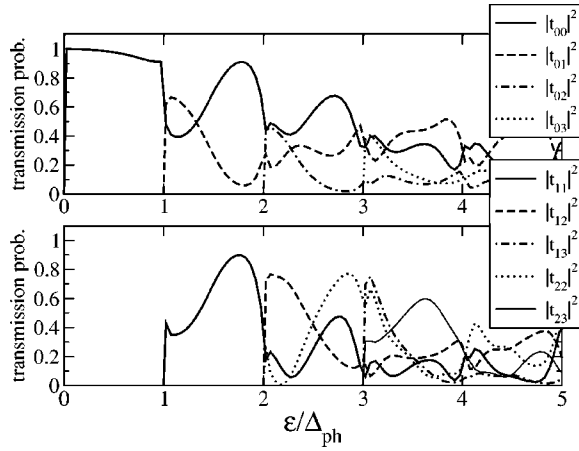


FIG. 9. Individual phonon transmission probabilities $|t_{mn}|^2$ as a function of energy for a circular right-angle bend with $R=1.00001b$.

inner radius of curvature, we have $R=1.00001b$, the transmission probabilities for which are shown in Fig. 9. The transmission probabilities when $R=1.00001b$ are similar to that for $R=1.001b$, shown previously in Fig. 6, as is the thermal conductance. We find in that in a $10\ \mu\text{m}$ Si-like quantum wire with $R=1.00001b$, the greatest suppression in G_{th} occurs near 2 mK and is again only about 0.5% of the conductance quantum in magnitude.

V. DISCUSSION

We have introduced a general method to calculate the transmission of scalar waves appropriate for mesoscopic electron and phonon transport through a curved wire or waveguide. Applications to electron transport accurately reproduce results obtained by other methods. Phonon transport through curved wires is considered.

Our results demonstrate that curvature hardly suppresses thermal transport, even for sharply bent wires, at least within the two-dimensional scalar phonon model considered. This behavior can, to some extent, be understood by considering transport in the extreme long- and short-wavelength limits. In the long-wavelength, low-energy limit, $T_{\text{ph}} \rightarrow 1$, a consequence of the rigid-body nature of the wire. T_{ph} also approaches unity for short wavelengths, because in this limit the phonons cannot sense the curvature.

Because the phonon reflection probability always vanishes in the long-wavelength limit, a simple perturbative (Born approximation) treatment is possible at low energies. For example, the energy-dependent $n=0$ transmission probability is

$$|t_{00}|^2 = 1 - |r_{00}|^2, \quad (47)$$

where, to leading nontrivial order,

$$r_{00} = -\frac{i\hbar v}{2\epsilon b} \int d^2R d^2R' e^{i\epsilon X/\hbar v} V_R G_0(\mathbf{R}, \mathbf{R}', \epsilon) V_{R'} e^{i\epsilon X'/\hbar v}. \quad (48)$$

V_R and $V_{R'}$ act on \mathbf{R} and \mathbf{R}' , respectively. This result allows the low-temperature thermal transport through a variety of

wire shapes to be addressed quite simply. Although an analogous perturbative expression can be derived for the electronic transmission probability as well, the form of the transverse part χ_n of the unperturbed scattering states, as dictated by the hard-wall boundary conditions, then leads to a divergence in the Born series,³³ consistent with the fact that $T_{\text{el}} \rightarrow 0$ in the long-wavelength limit.

We conclude with a brief discussion of the experimental implications of our mesoscopic thermal transport results, the charge-transport case having already been discussed in the literature.^{25,34} Thermal transport in carbon nanotubes has been studied experimentally by several groups,^{35–37} and nanotubes would be interesting systems to use to investigate the effects of bending on transport. To apply our method of analysis to this system would require the consideration of scattering of elastic waves in a curved, hollow tube. Although they were obtained for scalar phonons in two-dimensional strips, our results do suggest that the effects of curvature will be small, if not completely negligible, in these systems.

ACKNOWLEDGMENTS

This work was supported by the National Science Foundation under CAREER Grant No. DMR-0093217 and NIRT Grant No. CMS-0404031, and by the Research Corporation. Acknowledgment is also made to the Donors of the American Chemical Society Petroleum Research Fund for partial support of this research. It is a pleasure to thank Miles Blencowe, Andrew Cleland, Dennis Clougherty, and Kelly Patton for useful discussions, and Aleksandar Milošević for his contributions at the beginning stages of this work.

APPENDIX: INTEGRALS INVOLVING PRODUCTS OF DIRAC DELTA FUNCTIONS AND STEP FUNCTIONS

Here we discuss integrals of the form

$$\int_{-\infty}^{\infty} dx F[\Theta(x)]\delta(x), \quad (A1)$$

where F is twice continuously differentiable, and $\Theta(x)$ and $\delta(x)$ are the unit step and Dirac delta functions, respectively. Integrals of the form (A1), which involve *products* of generalized functions, depend sensitively on how $\Theta(x)$ and $\delta(x)$ are defined. It will be necessary to define $\Theta(x)$ and $\delta(x)$ according to their appearance in this work.

The step function $\Theta(x)$ appearing in Eq. (A1) originated from the curvature profile of Eq. (42) used to describe a circular segment of wire connected to a straight lead, and the delta function comes from its derivative with respect to arclength in Eq. (43), which is required by the effective potential V of Eq. (21). Therefore we require $\Theta(x)$ to be smooth (on some microscopic scale) and continuous, and $\delta(x)$ to be related to it by

$$\frac{d}{dx}\Theta(x) = \delta(x). \quad (A2)$$

We also require, of course, that

$$\lim_{x \rightarrow -\infty} \Theta(x) = 0 \quad \text{and} \quad \lim_{x \rightarrow \infty} \Theta(x) = 1. \quad (\text{A3})$$

The precise shape of $\Theta(x)$ near $x=0$ is immaterial, but with no loss of generality we can require that $\Theta(0) = \frac{1}{2}$.

Integrals of the form (A1) are now well defined. For example,

$$\int_{-\infty}^{\infty} dx \Theta(x) \delta(x) = \frac{1}{2}, \quad (\text{A4})$$

as expected, but

$$\int_{-\infty}^{\infty} dx [\Theta(x)]^2 \delta(x) = \frac{1}{3}, \quad (\text{A5})$$

instead of $\frac{1}{4}$. These results are obtained by integrating by parts and using the behavior of $\Theta(x)$ as $x \rightarrow \pm\infty$, *not* by evaluating $\Theta(0)$ and $[\Theta(0)]^2$. More generally,

$$\int_{-\infty}^{\infty} dx [\Theta(x)]^n \delta(x) = \frac{1}{n+1} \quad (\text{for } n > 0) \quad (\text{A6})$$

which is different from the naive value of $[\Theta(0)]^n = (\frac{1}{2})^n$, unless $n=1$.

The reason why

$$\int_{-\infty}^{\infty} dx F[\Theta(x)] \delta(x) \neq F[\Theta(0)] \quad (\text{A7})$$

in some of these examples is because the delta function is distributed over a small but finite region of x , whereas $\Theta(x)$ and $F[\Theta(x)]$ are generally *not* slowly varying over that length scale. We conclude, therefore, that integrals of the form (A1) appearing in the evaluation of matrix elements of V , have to be evaluated using integration-by-parts (or with an equivalent method).

- ¹T. S. Tighe, J. M. Worlock, and M. L. Roukes, *Appl. Phys. Lett.* **70**, 2687 (1997).
- ²M. L. Roukes, *Physica B* **263**, 1 (1999).
- ³K. Schwab, E. A. Henriksen, J. M. Worlock, and M. L. Roukes, *Nature (London)* **404**, 974 (2000).
- ⁴C. S. Yung, D. R. Schmidt, and A. N. Cleland, *Appl. Phys. Lett.* **81**, 31 (2002).
- ⁵A. N. Cleland, *Foundations of Nanomechanics* (Springer-Verlag, Berlin, 2002).
- ⁶C. W. J. Beenakker and H. van Houten, in *Solid State Physics: Advances in Research and Applications*, edited by H. Ehrenreich and D. Turnbull (Academic Press, New York, 1991), Vol. 44.
- ⁷S. Datta, *Electronic Transport in Mesoscopic Systems* (Cambridge University Press, Cambridge, 1997).
- ⁸N. Nishiguchi, Y. Ando, and M. N. Wybourne, *J. Phys.: Condens. Matter* **9**, 5751 (1997).
- ⁹L. G. C. Rego and G. Kirczenow, *Phys. Rev. Lett.* **81**, 232 (1998).
- ¹⁰D. E. Angelescu, M. C. Cross, and M. L. Roukes, *Superlattices Microstruct.* **23**, 673 (1998).
- ¹¹M. P. Blencowe, *Phys. Rev. B* **59**, 4992 (1999).
- ¹²A. Kambili, G. Fagas, V. I. Fal'ko, and C. J. Lambert, *Phys. Rev. B* **60**, 15 593 (1999).
- ¹³A. Buldum, D. M. Leitner, and S. Ciraci, *Europhys. Lett.* **47**, 208 (1999).
- ¹⁴D. M. Leitner and P. G. Wolynes, *Phys. Rev. E* **61**, 2902 (2000).
- ¹⁵M. P. Blencowe and V. Vitelli, *Phys. Rev. A* **62**, 052104 (2000).
- ¹⁶A. Ozpineci and S. Ciraci, *Phys. Rev. B* **63**, 125415 (2001).
- ¹⁷M. C. Cross and R. Lifshitz, *Phys. Rev. B* **64**, 085324 (2001).
- ¹⁸B. A. Glavin, *Phys. Rev. Lett.* **86**, 4318 (2001).
- ¹⁹D. H. Santamore and M. C. Cross, *Phys. Rev. Lett.* **87**, 115502 (2001).
- ²⁰K. R. Patton and M. R. Geller, *Phys. Rev. B* **64**, 155320 (2001).
- ²¹A. N. Cleland, D. R. Schmidt, and C. S. Yung, *Phys. Rev. B* **64**, 172301 (2001).
- ²²Q.-F. Sun, P. Yang, and H. Guo, *Phys. Rev. Lett.* **89**, 175901 (2002).
- ²³It will be sufficient to assume that the curves $\mathbf{r}(s)$ defining the edges of the wire as a function of arclength s are of class C^2 (derivatives through second order exist and are continuous).
- ²⁴The two-dimensional Helmholtz equation is valid at energy scales considerably less than v/d , where d is the thickness of the wire in the z direction.
- ²⁵J. T. Londergan, J. P. Carini, and D. P. Murdock, *Binding and Scattering in Two-Dimensional Systems: Applications to Quantum Wires, Waveguides, and Photonic Crystals* (Springer-Verlag, Berlin, 1999).
- ²⁶P. Exner and P. Seba, *J. Math. Phys.* **30**, 2574 (1989).
- ²⁷J. Goldstone and R. L. Jaffe, *Phys. Rev. B* **45**, 14 100 (1992).
- ²⁸Our method, of course, has its own limitations. For example, in the present formulation the width of the wire is assumed to be constant.
- ²⁹L. Lewin, *Theory of Waveguides* (John Wiley and Sons, New York, 1975).
- ³⁰R. E. Collin, *Field Theory of Guided Waves*, 2nd ed. (IEEE Press, New York, 1991).
- ³¹F. Sols and M. Macucci, *Phys. Rev. B* **41**, 11 887 (1990).
- ³²K. Lin and R. L. Jaffe, *Phys. Rev. B* **54**, 5750 (1996).
- ³³We thank Aleksandar Milošević for this observation.
- ³⁴H. U. Baranger, *Phys. Rev. B* **42**, 11 479 (1990).
- ³⁵J. Hone, M. Whitney, C. Piskoti, and A. Zettl, *Phys. Rev. B* **59**, R2514 (1999).
- ³⁶P. Kim, L. Shi, A. Majumdar, and P. L. McEuen, *Phys. Rev. Lett.* **87**, 215502 (2001).
- ³⁷D. J. Yang, Q. Zhang, G. Chen, S. F. Yoon, J. Ahn, S. G. Wang, Q. Zhou, Q. Wang, and J. Q. Li, *Phys. Rev. B* **66**, 165440 (2002).